DOI: 10.1002/JLB.3A0720-422R

JLB JOURNAL OF LEUKOCYTE BIOLOGY

ARTICLE

Different glycoforms of alpha-1-acid glycoprotein contribute to its functional alterations in platelets and neutrophils

Mosale Seetharam Sumanth[1] | Shancy P. Jacob[2] | Kandahalli Venkataranganayaka Abhilasha[1] | Bhanu Kanth Manne[3] | Venkatesha Basrur[6] | Sylvain Lehoux[7] | Robert A. Campbell[3] | Christian C. Yost[3,8] | Thomas M. McIntyre[9] | Richard D. Cummings[7] | Andrew S. Weyrich[3] | Matthew T. Rondina[3,4,5] | Gopal K Marathe[1,10]

[1]Department of Studies in Biochemistry, University of Mysore, Manasagangothri, Mysuru, Karnataka, India

[2]Department of Pediatrics, Division of Allergy and Immunology, University of Utah, Salt Lake City, Utah, USA

[3]Molecular Medicine Program, and Department of Internal Medicine and Pathology, University of Utah, Salt Lake City, Utah, USA

[4]The Geriatric Research Education and Clinical Center, Salt Lake City, Utah, USA

[5]Department of Internal Medicine, George E. Wahlen VAMC, Salt Lake City, Utah, USA

[6]Department of Pathology, University of Michigan Medical School, Ann Arbor, Michigan, USA

[7]Beth Israel Deaconess Medical Center, Department of Surgery, Harvard Medical School, Boston, Massachusetts, USA

[8]Department of Pediatrics, University of Utah, Salt Lake City, Utah, USA

[9]Department of Cardiovascular & Metabolic Sciences, Cleveland Clinic Lerner Research Institute, Cleveland, Ohio, USA

[10]Department of Studies in Molecular Biology, University of Mysore, Manasagangothri, Mysuru, Karnataka, India

Correspondence
Gopal K. Marathe, Department of Studies in Biochemistry, University of Mysore, Manasagangothri, Mysuru 570006, Karnataka, India.
Email: marathe1962@gmail.com

Abstract

Alpha-1-acid glycoprotein (AGP-1) is a positive acute phase glycoprotein with uncertain functions. Serum AGP-1 (sAGP-1) is primarily derived from hepatocytes and circulates as 12–20 different glycoforms. We isolated a glycoform secreted from platelet-activating factor (PAF)-stimulated human neutrophils (nAGP-1). Its peptide sequence was identical to hepatocyte-derived sAGP-1, but nAGP-1 differed from sAGP-1 in its chromatographic behavior, electrophoretic mobility, and pattern of glycosylation. The function of these 2 glycoforms also differed. sAGP-1 activated neutrophil adhesion, migration, and neutrophil extracellular traps (NETosis) involving myeloperoxidase, peptidylarginine deiminase 4, and phosphorylation of ERK in a dose-dependent fashion, whereas nAGP-1 was ineffective as an agonist for these events. Furthermore, sAGP-1, but not nAGP-1, inhibited LPS-stimulated NETosis. Interestingly, nAGP-1 inhibited sAGP-1-stimulated neutrophil NETosis. The discordant effect of the differentially glycosylated AGP-1 glycoforms was also observed in platelets where neither of the AGP-1 glycoforms alone stimulated aggregation of washed human platelets, but sAGP-1, and not nAGP-1, inhibited aggregation induced by PAF or ADP, but not by thrombin. These functional effects of sAGP-1 correlated with intracellular cAMP accumulation and phosphorylation of the protein kinase A substrate vasodilator-stimulated phosphoprotein and reduction of Akt, ERK, and p38 phosphorylation. Thus, the sAGP-1 glycoform limits platelet reactivity, whereas nAGP-1 glycoform also limits proinflammatory actions of sAGP-1. These studies identify new functions for this acute phase glycoprotein and demonstrate that the glycosylation of AGP-1 controls its effects on 2 critical cells of acute inflammation.

KEYWORDS

acute phase proteins, inflammation, neutrophil activation, NETosis, platelet aggregation

Abbreviation: DEAE-cellulose, diethyl aminoethane-cellulose; MPO, myeloperoxidase; nAGP-1, neutrophil derived AGP-1; PAD4, peptidylarginine deiminase 4; PAF, platelet-activating factor; PKA, protein kinase A; PRP, platelet-rich plasma; sAGP-1, serum Alpha-1-acid glycoprotein; VASP, vasodilator stimulated phosphoprotein.

Received: 3 July 2020 | Revised: 18 September 2020 | Accepted: 30 September 2020

 ©2020 Society for Leukocyte Biology

1 | INTRODUCTION

Alpha-1-acid glycoprotein (AGP-1) is a positive acute phase glycoprotein with a carbohydrate content contributing to 45% of its total mass. Hepatic synthesis of AGP-1 increases during an inflammatory response[1,2] and is released to the circulation (serum AGP-1; sAGP-1). Although numerous activities like immunomodulation and altering inflammatory milieu have been ascribed to AGP-1,[2,3] its function(s) are ill defined. Other cell types including human breast epithelial cells, lymphocytes, and monocytes secrete AGP-1 in response to appropriate inflammatory stimuli.[3–5] In addition, human neutrophils secrete AGP-1 in response to platelet-activating factor (PAF), LPS, TNF, and PMA.[6] AGP-1 undergoes extensive glycosylation and approximately 12–20 different glycoforms of AGP-1 are present in human blood.[2,7] This may be an underestimate, as more recent studies indicated that more than 150 isoforms of AGP-1 can occur in human plasma.[8,9]

This impressive number of glycoforms of AGP-1 is altered during both acute and chronic inflammation.[5,10–13] There is ample evidence to support the concept that the glycosylation pattern and degree of chain branching may serve as one of the markers for specific disease conditions.[3,9,10,12–17] Unraveling AGP-1 function(s), in general, remains challenging. For example, AGP-1 offers nonspecific protection against various Gram-negative bacterial infection and TNF-induced lethality,[18–20] but also promotes monocytes to an anti-inflammatory M2 phenotype rendering them ineffective against bacterial infections.[21] Furthermore, AGP-1 inhibits neutrophil migration in sepsis,[22] contributing to infection. More recently, Higuchi et al.[23] have shown that AGP-1 is also involved in the allograft rejection after kidney transplantation.

Additionally, AGP-1 is shown to have antiheparin effect leading to declined anticoagulation of blood.[24] Elevated levels of AGP-1 is correlated with increased incidence of ischemic stroke and carotid plaques.[25] AGP-1 is shown to interact with plasminogen activator inhibitor type I and stabilizes its activity and is shown to induce platelet shape change and activation, with an impact on thrombosis.[26,27] Contradicting to this, AGP-1 is shown to be a potent inhibitor of platelet aggregation, shown to have antithrombotic activity and offers protection against ischemia/reperfusion injury by preventing apoptosis and inflammation.[20,28–30]

Earlier studies have shown that activated TLR-4 triggers prothrombotic effects and that TLR-4 signaling is a potential therapeutic target.[31–34] In accordance to this, we previously observed that sAGP-1 preferentially inhibits the TLR-4 agonist bacterial LPS, but not TLR-2 agonist Braun Lipoprotein mediated inflammatory responses both in vivo and in vitro.[35,36] The main aim of this study is to understand the effect of 2 different glycoforms of AGP-1 on 2 different cell types of innate immune system. Accordingly, we show that the hepatocyte-derived sAGP-1 is proinflammatory, whereas the neutrophil-derived glycoforms (nAGP-1) primarily display anti-inflammatory activity. As the protein sequences of 2 glycoforms are identical but not the glycan structure, we conclude that different glycoforms differently contributes to the inflammatory milieu and may partly be responsible for the contradictory roles of this acute-phase glycoprotein.

2 | MATERIALS AND METHODS

2.1 | Chemicals

Cibacron F3GA agarose, DEAE-cellulose gel beads, anti-human AGP-1 antibody (A5566), anti-mouse-IgG-HRP antibody, commercial AGP-1, FBS, LPS, recombinant IL-8, micrococcal DNase, ADP, thrombin, apyrase, PGE_1, medium-199, poly-L-lysine, HBSS, and RPMI media were procured from Sigma Chemicals Co., St. Louis, MO, USA. Phospho-specific antibodies to p38, JNK, ERK, vasodilator-stimulated phosphoprotein (VASP), β-actin, and anti-rabbit IgG-HRP were obtained from Cell Signaling Technology, Danvers, MA, USA. Neutrophil extracellular traps (NETosis) marker antibodies, that is, citrullinated histone H3, histone H3, PAD4, and myeloperoxidase (MPO) antibodies were procured from Abcam, Cambridge, UK. Complete Mini EDTA-free protease inhibitor cocktail tablets were from Roche Diagnostics, Mannheim, Germany. PVDF membrane was from BioRad Laboratories, Hercules, CA, USA and thioglycolate media was obtained from Sisco Research Laboratories, Mumbai, India. Trypsin was purchased from Promega, Madison, WI, USA. Sytox green, Sytox orange, Syto green, Calcein 2 AM, and molecular weight markers were procured from Invitrogen, Carlsbad, CA, USA. Collagen was from Chronolog, Havertown, PA, USA. PAF was from Avanti polar Lipids, Alabaster, AL, USA. All the reagents used in the Glycomics mass spectrometry studies were procured from Sigma–Aldrich Co. except for PNGaseF, which was from New England Biolabs, Ipswich, MA, USA.

2.2 | Serum collection

Blood was drawn from healthy volunteers with informed consent. Permission to draw blood was obtained from the Institutional Human Ethics Committee, University of Mysore, Mysuru (UOM No. 104 Ph.D/2015-16). Briefly, the blood was collected and coagulated blood was then centrifuged at 600 *g* for 20 min at 25°C to collect serum and stored at −20°C till further use. All the experiments involving human blood were approved by the Institutional Human Ethics Committees of University of Mysore and University of Utah.

2.3 | Isolation of polymorphonuclear leukocytes (neutrophils)

Neutrophils were routinely isolated by dextran sedimentation and separated by centrifugation over Ficoll density gradient.[37] Neutrophil-rich pellets from this gradient were suspended in 1 ml of HBSS containing 0.2% human serum albumin (HBSS/A). Neutrophil isolation was also carried out by AutoMACS. Briefly, whole blood was labeled with CD15 microbeads and the neutrophils were positively selected using AutoMACS. (Miltenyi Biotech, San Diego, CA, USA)

2.4 | Secretion of AGP-1 from isolated human neutrophils

Ten million freshly isolated human neutrophils were stimulated or not with PAF (10^{-6} M), LPS (1 μg/ml), TNF (1,000 U/ml), and PMA (5 μg/ml)

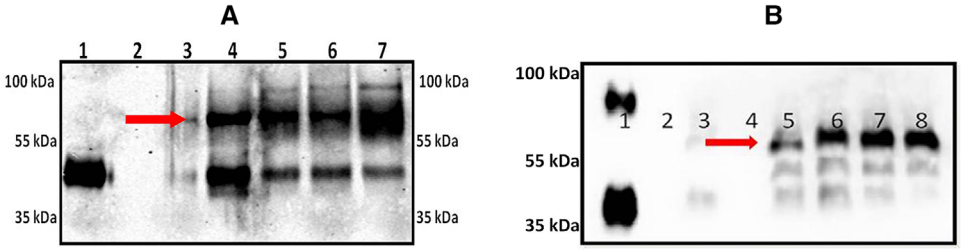

FIGURE 1 Stimulated human neutrophils secrete AGP-1 that differs from sAGP-1: (A) freshly isolated human neutrophils secrete AGP-1 after stimulation (for 60 min). Secreted proteins were concentrated, resolved, and immunoblotted against AGP-1. Lanes represent: lane 1, sAGP-1 (250 ng); lanes 2–7, nAGP-1 secreted from 2, 0 min control neutropils; 3, 60 min control neutrophils; 4, PAF (10^{-6} M) stimulated neutrophils; 5, TNF (1,000 U/ml) stimulated neutrophils; 6, LPS (1 μg/ml) stimulated neutrophils; 7, PMA (5 μg/ml) stimulated neutrophils. (B) Secretion of nAGP-1 by PAF stimulated neutrophils; lane 1, commercial AGP-1 (250 ng); 2, 0 min control; 3, 60 min control; 4, empty well; 5, PAF (10^{-4} M); 6, PAF (10^{-6} M); 7, PAF (10^{-8} M); 8, PAF (10^{-10} M). nAGP-1 is indicated by red arrow

for 60 min at 37°C. In parallel, human neutrophils were stimulated with varied concentrations of PAF (10^{-4} to 10^{-10} M) for 60 min at 37°C. Neutrophil supernatants derived under these conditions were concentrated and were immunoblotted against anti-human AGP-1 monoclonal antibody with controls at both "0 min" and at "60 min." sAGP-1 (250 ng) isolated previously in our laboratory[35] was used as the reference standard, as commercial AGP-1 many times displayed variation in electrophoretic mobility (Fig. 1B).

2.5 | Purification of AGP-1 from neutrophil supernatant

Purification of AGP-1 from PAF-stimulated neutrophil supernatants was carried out as described earlier.[35] Briefly, pooled neutrophil supernatants were loaded on to a Cibacron F3GA agarose column (10 × 1.5 cm) equilibrated with 10 mM phosphate buffer (pH 7.8). Unbound proteins containing AGP-1 were eluted at a flow rate of 1 ml/min. AGP-1 containing fractions were pooled and concentrated. The concentrate was then applied to a DEAE-cellulose column (25 × 0.5 cm) equilibrated with 30 mM acetate buffer (pH 5.0). Fractions were eluted with a sodium chloride gradient (0–2 M) at a flow rate of 24 ml/h. AGP-1 containing fractions were pooled, concentrated, and quantified for protein using Lowry's method.[38] The endotoxin content of purified AGP-1 was assessed by Limulus amebocyte lysate (LAL) assay (Endochrome – K^{TM}; Charles River, Wilmington, MA, USA) as per manufacturer's instructions.

2.6 | Western blotting for AGP-1

AGP-1 samples were resolved on a reducing SDS-PAGE (7.5% acrylamide) and visualized by Western blotting. Blots were stained using appropriate primary antibody (anti-human AGP-1 monoclonal antibody; 1:10,000 v/v) and secondary antibody (anti-mouse IgG HRP conjugate; 1:5,000 v/v). The blots were visualized using freshly prepared ECL reagent by UV-transillumination (Uvi-Tech, Cambridge, UK).

2.7 | Protein mass spectrometry analysis

Purified samples were resolved by SDS-PAGE, visualized using Coomassie stain; AGP-1 band was excised and destained with 30% methanol for 4 h. Upon reduction (10 mM dithiothreitol) and alkylation (65 mM 2-chloroacetamide) of the cysteines, protein was digested overnight with sequencing grade-modified trypsin. The resulting peptides were resolved on a nanocapillary reverse phase column (Acclaim PepMap C18, 2 micron, 50 cm; Thermo Scientific, Madison, WI, USA) using a 1% acetic acid/acetonitrile gradient at 300 nl/min and directly introduced into Q Exactive HF mass spectrometer (Thermo Scientific, Madison, WI, USA). MS1 scans were acquired at 60 K resolution (AGC target = 3e6, max IT = 50 ms). Data-dependent high-energy C-trap dissociation MS/MS spectra were acquired for the 20 most abundant ions (Top20) following each MS1 scan (15 K resolution; AGC target = 1e5; relative CE ~28%). Proteome Discoverer (V 2.1; Thermo Scientific) software suite was used to identify the peptides by searching the HCD data against an appropriate database. Search parameters included MS1 mass tolerance of 10 ppm and fragment tolerance of 0.1 Da. False discovery rate (FDR) was determined using Fixed PSM validator and proteins/peptides with a FDR of ≤1% were retained for further analysis.

2.8 | Glycomics mass spectrometry analysis

Coomassie-stained AGP-1 protein bands were excised, washed with 400 μl of 50 mM AMBIC (ammonium bicarbonate) in 50% acetonitrile, dried and 200 μl of 10 mM DTT (1,4-dithiothreitol) solution in 50 mM AMBIC were added and incubated at 50°C for 30 min. The gel was washed with 200 μl of acetonitrile and dried. The samples were incubated with 200 μl of 55 mM IAA (iodoacetamide) in 50 mM AMBIC for 30 min at room temperature in dark. The samples were again washed with 500 μl of 50 mM AMBIC for 15 min at room temperature followed by a wash with 200 μl of acetonitrile for 5 min. The samples were dried prior to adding 500 μl of 50 mM AMBIC containing 10 μg of TPCK-treated trypsin and incubated overnight at 37°C. The tryptic digestion was terminated and supernatants were recovered. Further peptides were recovered by 2 cycles of washes with 200 μl of 50 mM AMBIC, 200 μl of 50% acetonitrile in 50 mM AMBIC, and 200 μl of acetonitrile. All supernatants and washes were pooled in the same glass tube used and lyophilized. The dried peptides were resuspended in 200 μl of 50 mM AMBIC and incubated overnight with 1 μl of PNGaseF at 37°C.

The enzymatic reaction was stopped by using 5% of acetic acid prior to purification of the released N-glycans over a C18 Sep-Pak (50 mg) column (Waters, Milford, MA, USA) conditioned with 1 column volume (CV) of methanol, 1 CV of 5% of acetic acid, 1 CV of 1-propanol, and 1 CV of 5% of acetic acid. The C18 column was washed with 3 ml of 5% of acetic acid. Flow through and wash fractions were collected, pooled, and lyophilized prior to permethylation. Lyophilized N-glycan samples were incubated with 1 ml of DMSO-NaOH slurry solution and 500 μl of methyl iodide for 30 min under shaking at 25°C. The reaction was stopped with 1 ml of Milli-Q water and 1 ml of chloroform was added to purify out the permethylated N-glycans. The chloroform layer was washed 3 times with 3 ml of Milli-Q water and dried. The dried materials were redissolved in 200 μl of 50% methanol prior to be loaded into a conditioned (1 CV methanol, 1 CV Milli-Q water, 1 CV acetonitrile, and 1 CV Milli-Q Water) C18 Sep-Pak (50 mg) column. The C18 column was washed with 15% acetonitrile and then eluted with 3 ml of 50% acetonitrile. The eluted fraction was lyophilized and then redissolved in 10 μl of 75% methanol from which 1 μl was mixed with 1 μl DHB (2,5-dihydroxybenzoic acid) (5 mg/ml in 50% acetonitrile with 0.1% trifluoroacetic acid) and spotted on a MALDI polished steel target plate (Bruker Daltonics, Germany). MS data were acquired on a Bruker UltraFlex II MALDI-TOF Mass Spectrometer instrument. Reflective positive mode was used and data recorded between 1,000 *m/z* and 5,000 *m/z*. For each MS N-glycan profiles the aggregation of 20,000 laser shots or more were considered for data extraction. Only MS signals matching a N-glycan composition were considered for further analysis. Subsequent MS post-data acquisition analysis were made using mMass.[39]

2.9 | Human neutrophil adhesion

For assessment of adhesion, the human neutrophil suspension (1×10^7 cells/ml) was loaded with Calcein-AM to a final concentration of 1 μM prior to incubation for 45 min at 37°C. The labeled neutrophils (1×10^6 cells/well) were incubated with sAGP-1 or nAGP-1 (25, 50, and 100 μg/ml) in triplicate wells in cell culture plates (Nest Biotechnology Co. Ltd., China) precoated with 0.2% gelatin. Unbound neutrophils were removed by washing twice with HBSS/A and the adherent neutrophils were visualized and photographed at a magnification of 10× by fluorescent microscopy (Motic BA410 fluorescence microscope, Hong Kong; with Nikon DS-Qi2 camera, Japan).[36] The number of cells adhered in each well was determined by counting the cells adhered in 10 randomly chosen fields using ImageJ software (ver.1.51j8) and then calculating the average number of cells adhered per field.

2.10 | Neutrophil migration

Neutrophil migration was assessed using Transwell plates (Costar, Corning Inc., NY, USA) with 5 μm pore size inserts. 1×10^6 (200 μl) freshly isolated neutrophils in M-199 medium were incubated in the upper chamber of the Transwell and the chemoattractant, IL-8 (10 ng/ml) and/ or AGP-1 (sAGP-1 and nAGP-1) (25, 50, and 100 μg/ml) were introduced in the lower chamber. The number of neutrophils migrating to the lower chamber after incubation for 1 h at 37 °C with 5% CO_2 were counted with a hemocytometer and expressed as % neutrophil-migrated using IL-8 as positive control (100% migration).

2.11 | Neutrophil degranulation and estimation of ROS

Neutrophil degranulation was monitored by the secretion/production of MPO by stimulated neutrophils. 1×10^6 freshly isolated neutrophils suspended in HBSS/A were treated with varying concentrations of sAGP-1 (25, 50, and 100 μg/ml) or nAGP-1 (25, 50, and 100 μg/ml) for 1 h at 37°C with 5% CO_2. LPS (10 μg/ml) was used as positive control. MPO activity was measured according to the method of Bradley et al.[40] Briefly, after the treatment, neutrophils were pelleted by centrifugation at 300 *g* for 5 min at 4°C. The supernatant was separated from the pellet. The neutrophils pellet was lysed using RIPA buffer containing protease inhibitor cocktail. Both the supernatant and the cell lysate were used as the source for MPO. Aliquots of the supernatant (250 μl) and cell lysate (50 μl) were mixed with 2.9 ml of 50 mM sodium phosphate buffer (pH 6.0) containing 167 μg/ml of o-dianisidine (SRL, Mumbai, India) and 0.0005% H_2O_2. The change in absorbance at 460 nm was recorded in an UV-Visible spectrophotometer (Biomate 3S; Thermo Scientific, Madison, WI, USA).

For ROS estimation, freshly isolated neutrophils (1×10^6) were treated with different concentrations (25, 50, and 100 μg/ml) of sAGP-1 or nAGP-1 for 1 h at 37°C with 5% CO_2. Again LPS (10 μg/ml) was taken as positive control. After treatment, the cells were washed and loaded with 20 μM DCF-DA and incubated in dark for 15 min. The fluorescence was measured at an excitation at 488 nm and emission at 525 nm in a multi-mode plate reader (Thermo Scientific, Madison, WI, USA).[41]

2.12 | Assessment and quantification of NETosis

One million freshly isolated human neutrophils were treated with LPS (10 μg/ml) in the presence/absence of AGP-1 (sAGP-1 and nAGP-1 glycoforms at 25, 50, and 100 μg/ml) before being transferred to poly-L-lysine-coated coverslips. The neutrophils were incubated at 37°C in 5% CO_2 for 1 h before adding Syto green (cell-permeable) and Sytox orange (cell-impermeable) fluorescent dye mixture and visualized by fluorescent microscopy (EVOS Fluorescence microscope; Thermo Scientific, Waltham, MA, USA). The 2 dye images were merged using ImageJ software (ver. 1.51j8).

High-throughput NET quantification[42] was employed to quantify neutrophil NETs. For this, 24 well plates were precoated with poly-L-lysine before neutrophil addition followed by stimulation for 1 h by indicated agonists at 37°C under 5% CO_2. The extracellular traps were recovered by treating the neutrophils with Micrococcal DNase and the DNA stained with cell-impermeable Sytox green dye. These were measured with a fluorescent plate-reader with excitation at 485 nm and emission at 530 nm. Parallelly, NETosis was also quantified by using

NETosis assay kit (ab 235979; Abcam). Activity of neutrophil elastase on harvested NET structures was quantified in this method according to the manufacturer's instructions.

2.13 | Profiling of protein markers of NETosis by Western blotting

Freshly isolated human neutrophils (1×10^6 cells/ml) were stimulated for 1 h with sAGP-1 (25, 50, and 100 μg/ml) and highest dose for nAGP-1 (100 μg/ml) with or without LPS (10 μg/ml). In some experiments, neutrophils were treated with a combination of sAGP-1 (50 μg/ml) and nAGP-1 (50 μg/ml). Unstimulated neutrophils served as the negative control. Lysates were prepared by using RIPA buffer containing protease inhibitor cocktail. Immunoblots were developed using specific primary and appropriate secondary antibodies for citrullinated histone H3 (R2, R8, and R17) (cit His H3), Histone H3, peptidylarginine deiminase (PAD) 4, MPO, phospho-pERK, and β-actin (1:1,000 v/v).

2.14 | Platelet aggregation using washed human platelets

Blood was drawn from healthy volunteers with informed consent. Platelet-rich plasma (PRP) was isolated from this blood using the method previously described by Zhou and Schmaier.[43] Briefly, blood was drawn into citrated tubes (1/9) and centrifuged for 15 min at 45 *g* at 25°C to obtain PRP. The PRP was treated with PGE_1 to stop the activation of platelets. PGE_1-treated PRP was centrifuged at 225 *g* for 20 min at 25°C without breaking. The resulting platelet pellet was resuspended in HEPES-Tyrode's buffer containing 0.02 U Apyrase. Platelet aggregation was performed by using 2×10^8 platelets/ml in a final reaction volume of 500 μl at 37°C with stirring at 1,200 rpm. All assays were performed using Chrono-log aggregometer and the traces were recorded using AGGRO/LINK 8 ver.1.0.1 software.

2.15 | Signaling by stimulated platelets

Washed platelets (2×10^8 cells/ml) were stimulated for 5 min with thrombin (0.075 U/assay), PAF (4 μM), or ADP (500 nM) with or without sAGP-1 (50 μg/ml). Unstimulated washed platelets served as the negative control. Lysates were prepared by using perchloric acid (6 N) and reducing sample buffer (modified Laemmli buffer). Immunoblots were developed using specific primary and appropriate secondary antibodies for phospho-p38, phospho-Akt, phospho-ERK, phospho-VASP (S157), and β-actin (1:1,000 v/v).

2.16 | ELISA for platelet cAMP

cAMP levels in washed platelets were quantified after treatment with buffer, thrombin (0.075 U/assay), ADP (500 nM), or PAF (4 μM) with or without sAGP-1 using competitive ELISA kit (EMSCAMPL; Invitrogen, Austria) according to the manufacturer's instructions.

2.17 | Statistical analysis

All experiments are a representative of at least 2 or more experiments. The data are represented as mean ± SEM. Analysis between 2 groups were performed using Student *t*-test. For analysis of more than 2 groups one-way ANOVA was used. All the statistical analyses were carried out using GraphPad Prism 5 software.

3 | RESULTS

3.1 | Neutrophils secrete distinct AGP-1 isoforms

To isolate the extrahepatic secretion of AGP-1, freshly isolated human neutrophils (1×10^6 cells/ml) (isolated by using both ficoll density gradient method and CD15 positive selection) were stimulated with the agonists PAF (10^{-6} M), TNF (1,000 U/ml), PMA (5 μg/ml), or LPS (1 μg/ml) and the secreted proteins were immunoblotted against AGP-1. Unstimulated neutrophils did not secrete detectable AGP-1, whereas neutrophils stimulated by these agonists did, suggesting the extrahepatic source of AGP-1 (Fig. 1A). Stimulated neutrophils, however, secreted both a 43 kDa AGP-1 corresponding to sAGP-1 and also released more slowly migrating (~60 kDa) larger form of AGP-1, which we termed nAGP-1 (Fig. 1B). The ratio of the 2 isoforms differed according to the inciting agonists. We sought to purify the higher molecular weight nAGP-1 isoform using conventional chromatographic techniques (see section *Materials and Methods*) and so stimulated neutrophils with PAF to obtain an AGP-1 corresponding to both sAGP-1 and nAGP-1. However, only the larger nAGP-1 was isolated by this purification protocol and was used for further experimentations. Based on immunodetection, we found that neutrophils stimulated with lower concentrations of PAF secreted higher amount of higher molecular weight (~60 kDa) nAGP-1 than higher concentrations of PAF (Fig. 1B).

In the next series of experiments, we determined the basis for the distinct physical properties of the 2 AGP-1 isoforms. Unlike sAGP-1, nAGP-1 failed to bind to the DEAE-cellulose anion exchange column and so eluted in the void volume of this chromatographic separation (Figs. 2A–2D), whereas sAGP-1 eluted at a salt concentration of 150 mM. The endotoxin content of both the purified nAGP-1 and sAGP-1 was <5 EU/mg protein, and so would not be relevant in subsequent biologic analyses. The slow moving nAGP-1 (~60 kDa) before purification (Fig. 1B), now moved faster than that of the 43 kDa sAGP-1 after purification (Fig. 2C) on SDS-PAGE, probably due to the dissociation of the "uncharacterized binding factor(s)" (see section *Discussion*).

3.2 | Glycan and peptide analysis of nAGP-1 by mass spectrometry

The electrophoretic mobility of purified nAGP-1 was slower than that of sAGP-1 before purification. To understand whether this reflects size or charge differences, we subjected the 2 isoforms to mass spectrometry analysis. We found the sequence of the 2 proteins aligned

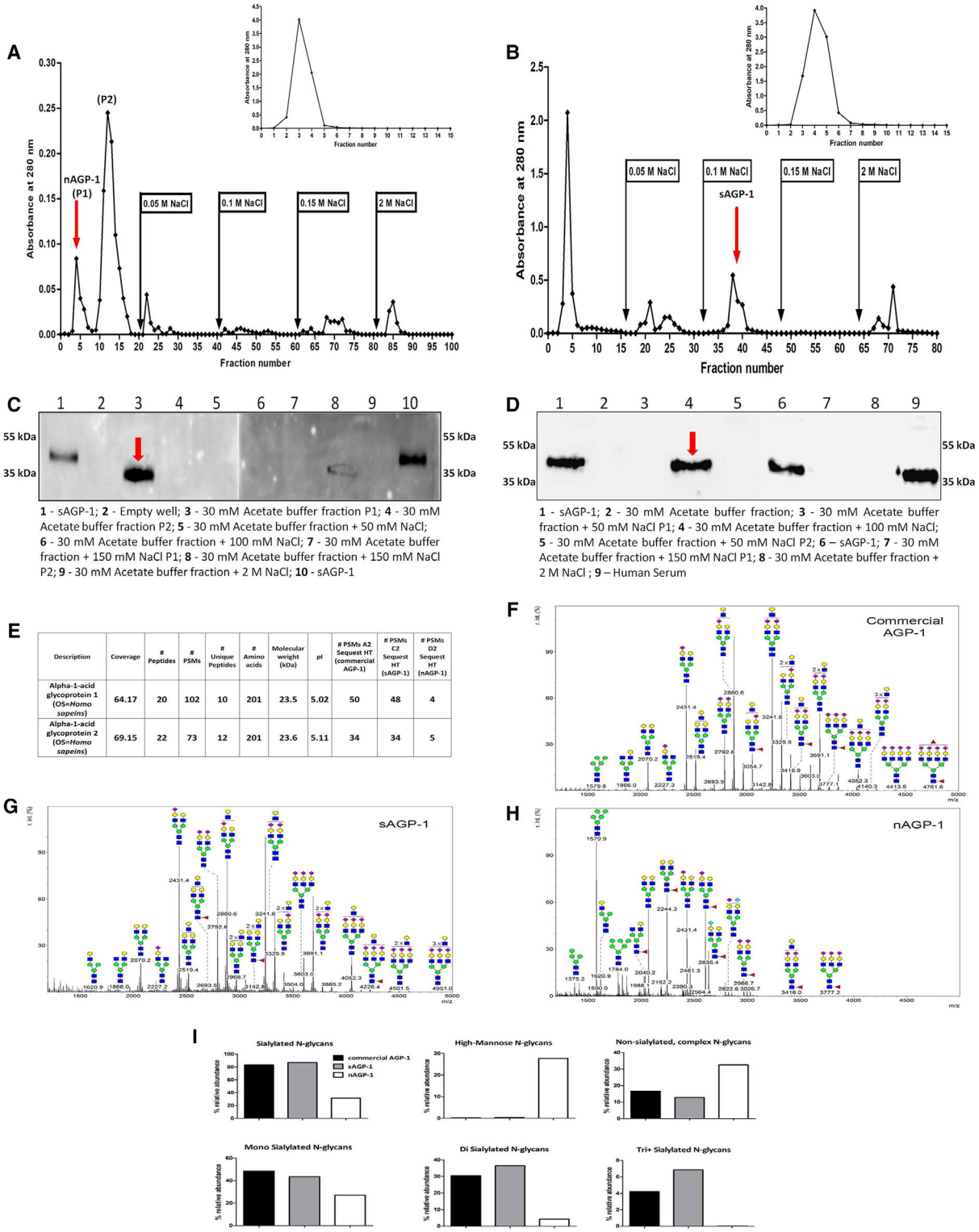

1 - sAGP-1; **2** - Empty well; **3** - 30 mM Acetate buffer fraction P1; **4** - 30 mM Acetate buffer fraction P2; **5** - 30 mM Acetate buffer fraction + 50 mM NaCl; **6** - 30 mM Acetate buffer fraction + 100 mM NaCl; **7** - 30 mM Acetate buffer fraction + 150 mM NaCl P1; **8** - 30 mM Acetate buffer fraction + 150 mM NaCl P2; **9** - 30 mM Acetate buffer fraction + 2 M NaCl; **10** - sAGP-1

1 - sAGP-1; **2** - 30 mM Acetate buffer fraction; **3** - 30 mM Acetate buffer fraction + 50 mM NaCl P1; **4** - 30 mM Acetate buffer fraction + 100 mM NaCl; **5** - 30 mM Acetate buffer fraction + 50 mM NaCl P2; **6** – sAGP-1; **7** - 30 mM Acetate buffer fraction + 150 mM NaCl P1; **8** - 30 mM Acetate buffer fraction + 2 M NaCl ; **9** – Human Serum

Description	Coverage	# Peptides	# PSMs	# Unique Peptides	# Amino acids	Molecular weight (kDa)	pI	# PSMs A2 Sequest HT (commercial AGP-1)	# PSMs C2 Sequest HT (sAGP-1)	# PSMs D2 Sequest HT (nAGP-1)
Alpha-1-acid glycoprotein 1 (OS=*Homo sapeins*)	64.17	20	102	10	201	23.5	5.02	50	48	4
Alpha-1-acid glycoprotein 2 (OS=*Homo sapeins*)	69.15	22	73	12	201	23.6	5.11	34	34	5

FIGURE 2 **Purification and characterization of nAGP-1 in comparison with sAGP-1**: elution profile of (A) PAF-induced neutrophil supernatant (nAGP-1) and (B) serum-derived AGP-1 (sAGP-1) on DEAE-cellulose column. The insets represent the elution profile of nAGP-1 (A inset) and sAGP-1 (B inset) on Cibacron blue column respectively. The fraction(s) containing the respective AGP-1 is indicated by red arrow. (C) and (D) Western blotting analysis of different fractions of DEAE-cellulose column against nAGP-1 and sAGP-1, respectively (2 different gels) indicated by red arrow. (E) Mass spectral analysis of commercial AGP-1, sAGP-1, and nAGP-1. The data revealed that the protein components of the 2 AGP-1s are identical. Glycomic analysis of (F) commercial AGP-1 and (G) sAGP-1 showed that these 2 preparations are similar. (H) nAGP-1 differed in glycosylation complexity and composition when compared with sAGP1.■, N-acetyl glucosamine;●, mannose;○, galactose;▲, fucose;◆, sialic acid. (I) % relative abundance of sialylated, nonsialylated, high-mannose, monosialylated, disialylated, and trisialylated N-glycans present in commercial AGP-1, sAGP-1, and nAGP-1

and generated peptides that were identical for the entire sequence (Fig. 2E). We next examined the glycosylation, more precisely the N-linked glycans (N-glycans) of sAGP-1 and nAGP-1. sAGP-1 is mainly glycosylated with complex biantennary and triantennary, sialylated N-glycan chains. 86% of sAGP-1 N-glycans are sialylated, with the majority of them being monosialylated and disialylated N-glycans (Figs. 2G and 2I). This is similar, if not identical, to commercially available, serum-derived AGP-1 (Figs. 2F and 2I). By contrast, nAGP-1 has different types of N-glycan. The relative abundance of complex sialylated N-glycans in nAGP-1 was significantly reduced (~31%), and these are mainly monosialylated N-glycans (Figs. 2H and 2I). High-mannose-type N-glycans are, however, much more relatively abundant among nAGP-1 N-glycans (~27%) compared with sAGP-1 and commercial AGP-1 N-glycans (<1% for both) (Figs. 2F–2I). As nAGP-1 differs from the sAGP-1 only with respect to N-glycans and not the protein core, we considered these as distinct glycoforms of AGP-1.

3.3 | AGP-1 glycoforms differently stimulate neutrophils

AGP-1 is elaborated in response to systemic inflammation, but with incompletely defined biologic effects. To determine whether either or both of the AGP-1 glycoforms contribute to the inflammatory responses, we determined whether their undefined functions include the ability to localize neutrophils to sites of inflammation. Neutrophils rapidly and avidly adhere in response to inflammatory stimuli.[44,45] To quantify this, we labeled neutrophils with Calcein, a fluorescent vital dye, and assessed adhesion to a gelatin-coated glass surface that prevents interaction with unstimulated neutrophils. We found both sAGP-1 and nAGP-1 were agonists for this event, with sAGP-1 ultimately stimulating twice the number of neutrophils to adhere than nAGP-1 (Figs. 3A and 3B). At lower concentrations, sAGP-1 also proved to be a significantly more potent agonist than nAGP-1. We next examined neutrophil chemotaxis using Transwell chambers to find migration in response to AGP-1 recapitulated adhesion, with sAGP-1 being significantly more potent and more stimulatory than nAGP-1 (Fig. 3C). Thus, although both glycoforms of AGP-1 are neutrophil agonists, quantitative examination showed that these glycoforms differently affect neutrophil function, with sAGP-1 acting as a more robust neutrophil chemoattractant than nAGP-1. Following this trend, sAGP-1, but not nAGP-1, induced ROS production (Fig. 3D) and MPO secretion (Figs. 3E and 3F) in a concentration-dependent manner.

3.4 | sAGP-1 induces NETosis, whereas nAGP-1 is inhibitory

Neutrophils extrude their DNA along with antimicrobial enzymes and peptides after encountering microbes or during inflammation that forms a net-like structure to entrap bacteria in a process termed NETosis.[46] We determined whether AGP-1s activate neutrophils to undergo NETosis to find sAGP-1, but not nAGP-1, induced this response (Fig. 4A). In fact, the highest concentration of sAGP-1 was comparable to the level of NETosis induced by the positive control LPS (Fig. 4B). The concentration–response relationship showed 50 μg/ml sAGP-1 was suboptimal, enabling us to determine the combined effect of sAGP-1 and nAGP-1 at this concentration. We found nAGP-1 at this concentration not only failed to induce NETosis, it inhibited the NETosis induced by sAGP-1 (Figs. 4A and 4B inset). Interestingly, sAGP-1 and not nAGP-1 suppressed LPS-induced NETosis in a concentration-dependent fashion (Figs. 4C and 4D), which is in accordance with our previous study.[35] nAGP-1, in contrast, failed to reduce LPS-induced NETosis even at 100 μg/ml, where sAGP-1 abolished the NETosis induced by LPS (Figs. 4C and 4D). We also validated NETosis by measuring the neutrophil elastase bound to the extracellular DNA in a parallel experiment (Fig. 5A).

3.5 | Analysis of markers of NETosis

To determine the molecular events in play during NETosis, citrullinated Histone H3 (cit His H3), PAD4, MPO, and phospho-ERK were monitored by immunoblotting as these are the key markers of NETosis.[47–49] We found that, the sAGP-1 showed a concentration-dependent increase in the expression of the key markers of NETosis, whereas nAGP-1 failed to increase the expression of these proteins significantly (Figs. 5B–5F). Furthermore, sAGP-1 (100 μg/ml), but not nAGP-1 (100 μg/ml), inhibited the LPS-induced expression of cit His H3, PAD4, MPO, and phosphorylation of ERK at the concentration tested. In accordance with the previous results (Figs. 4B inset and 5A), at submaximal concentration nAGP-1 (50 μg/ml) inhibited sAGP-1 (50 μg/ml)-induced expression of these proteins (Figs. 5B–5F). Moreover, as sAGP-1 induced phosphorylation of ERK and ROS production (Fig. 3D), sAGP-1 likely induces NETosis via Raf-MEK-ERK pathway.

3.6 | sAGP-1, but not nAGP-1, suppresses platelet aggregation induced by incomplete stimuli

To understand whether AGP-1 affect platelets, we examined aggregation of washed human platelets incubated with AGP-1 alone or together with thrombocyte agonists. We found neither of the AGP-1 glycoforms stimulated platelet aggregation by themselves (Fig. 6A inset). Instead, sAGP-1 profoundly suppressed, and ultimately abolished, platelet aggregation induced by either PAF (Figs. 6A, 6E, and 6F) or ADP (Figs. 6B, 6G, and 6H). In contrast, nAGP-1 was without effect on stimulated platelet aggregation. Platelet aggregation in response to the single "strong" platelet agonist thrombin, however, was not affected by either of the AGP-1 glycoforms (Figs. 6C, 6I, and 6J), whereas soluble collagen acting on non-G protein-coupled receptors was only modestly affected (Figs. 6D, 6K, and 6L).

3.7 | sAGP-1 stimulates cAMP accumulation in platelets stimulated by incomplete agonists

To understand the molecular mechanism underlying sAGP-1 inhibition of platelet aggregation, we assessed the effect of sAGP-1 on cAMP, whose levels profoundly affect platelet aggregation. We

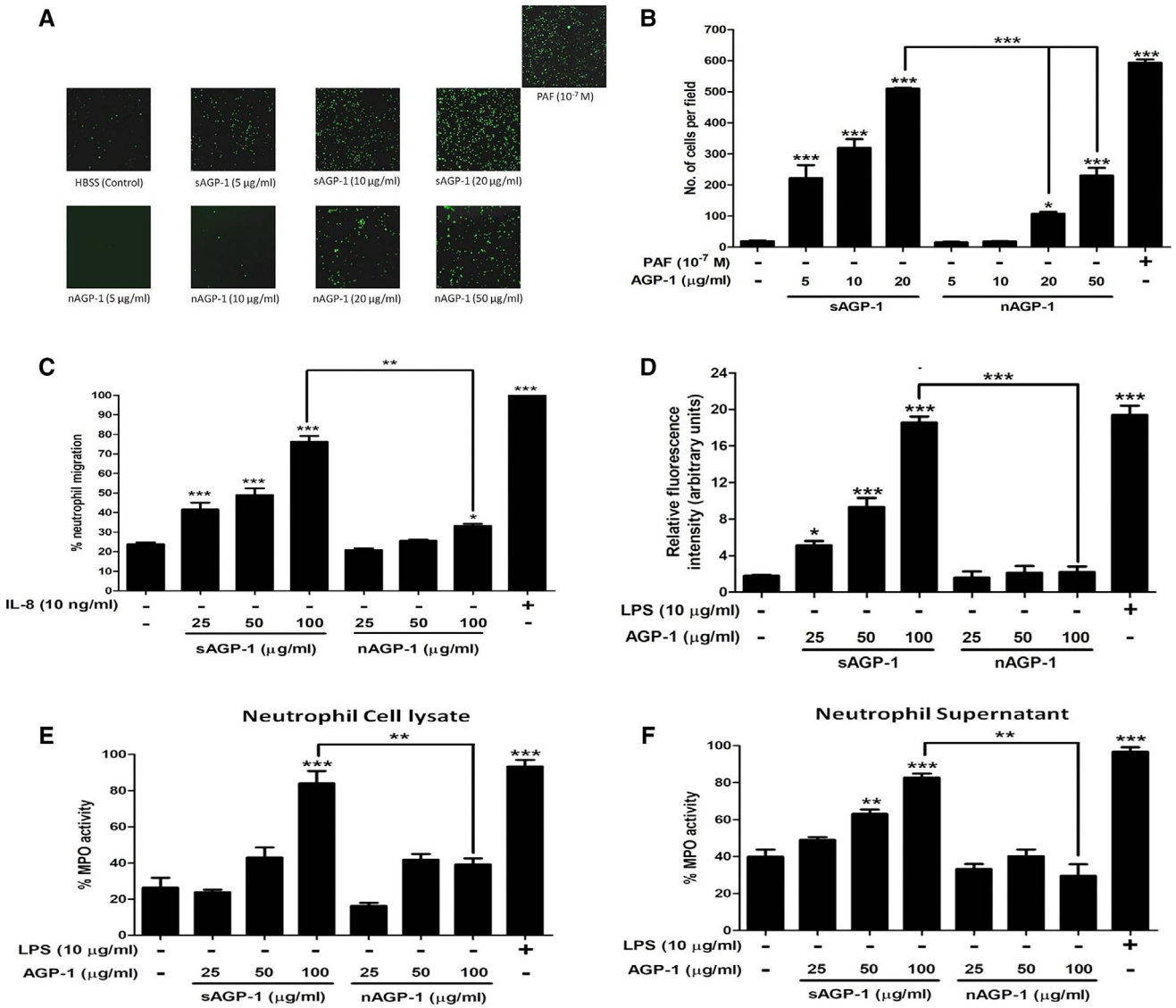

FIGURE 3 **sAGP-1 is more potent activator of human neutrophils than nAGP-1**: (A) neutrophil adhesion. Neutrophils loaded with Calcein-AM in HBSS/A were treated with increasing concentrations of sAGP-1 and nAGP-1(5–50 μg/ml) separately. The adherent PMNs were visualized under fluorescence microscope at a magnification of 10×. PAF (10^{-7} M) was used as positive control. (B) Quantitation of neutrophils adhesion. AGP-1-induced PMN activation was quantified by counting the cells per field using ImageJ software as explained under section "*Materials and Methods*." (C) Neutrophil migration. Chemotaxis in response to sAGP-1 and nAGP-1 (25, 50, and 100 μg/ml) was tested using Transwell plates with 5 μm pore size inserts (Boyden chamber assay). IL-8 (10 ng/ml) served as the positive control. Percentage of neutrophils migrated to the lower chamber were calculated and plotted. Chemotaxis induced in response to IL-8 was considered 100%. (D) ROS production. Freshly isolated neutrophils were treated with LPS (10 μg/ml), different concentrations (25, 50, and 100 μg/ml) of sAGP-1 or nAGP-1 for 1 h at 37°C with 5% CO_2. After treatment, the cells were washed; loaded with DCF-DA and the fluorescence was measured using fluorescence multimode plate reader (E and F) MPO secretion. Neutrophils were stimulated with various concentrations (25, 50, and 100 μg/ml) of sAGP-1 or nAGP-1. Both neutrophils cell lysate (E) and supernatant (F) were used to assess the MPO activity as described in section "*Materials and Methods*." LPS (10 μg/ml) served as positive control, whereas unstimulated neutrophils served as negative control. The data shown are mean ± SEM. ***$P < 0.0001$, **$P < 0.001$, and *$P < 0.01$ as determined one-way ANOVA

found sAGP-1 modestly, but not significantly, reduced cAMP levels in resting platelets, whereas the strong agonist thrombin significantly reduced cAMP abundance (Fig. 7A). sAGP-1 did not affect thrombin-suppressed cAMP, but did greatly increase cAMP levels in platelets stimulated with either PAF or ADP. We next determined whether sAGP-1 affected kinase signaling, and visualized the phosphorylation status of Akt, p38, and ERK kinases as well as the actin regulator VASP that is phosphorylated by cAMP and protein kinase A (PKA). The phosphoblot of platelets stimulated in the presence or absence of sAGP-1 showed that thrombin stimulation, like aggregation, was unaffected by this acute phase protein (Figs. 7B–7F). These experiments also demonstrated that VASP phosphorylation was increased by sAGP-1 when cAMP levels increased (Figs. 7A, 7B, and 7F). In contrast, phosphorylation and activation of serine kinases by PAF or ADP was reduced by

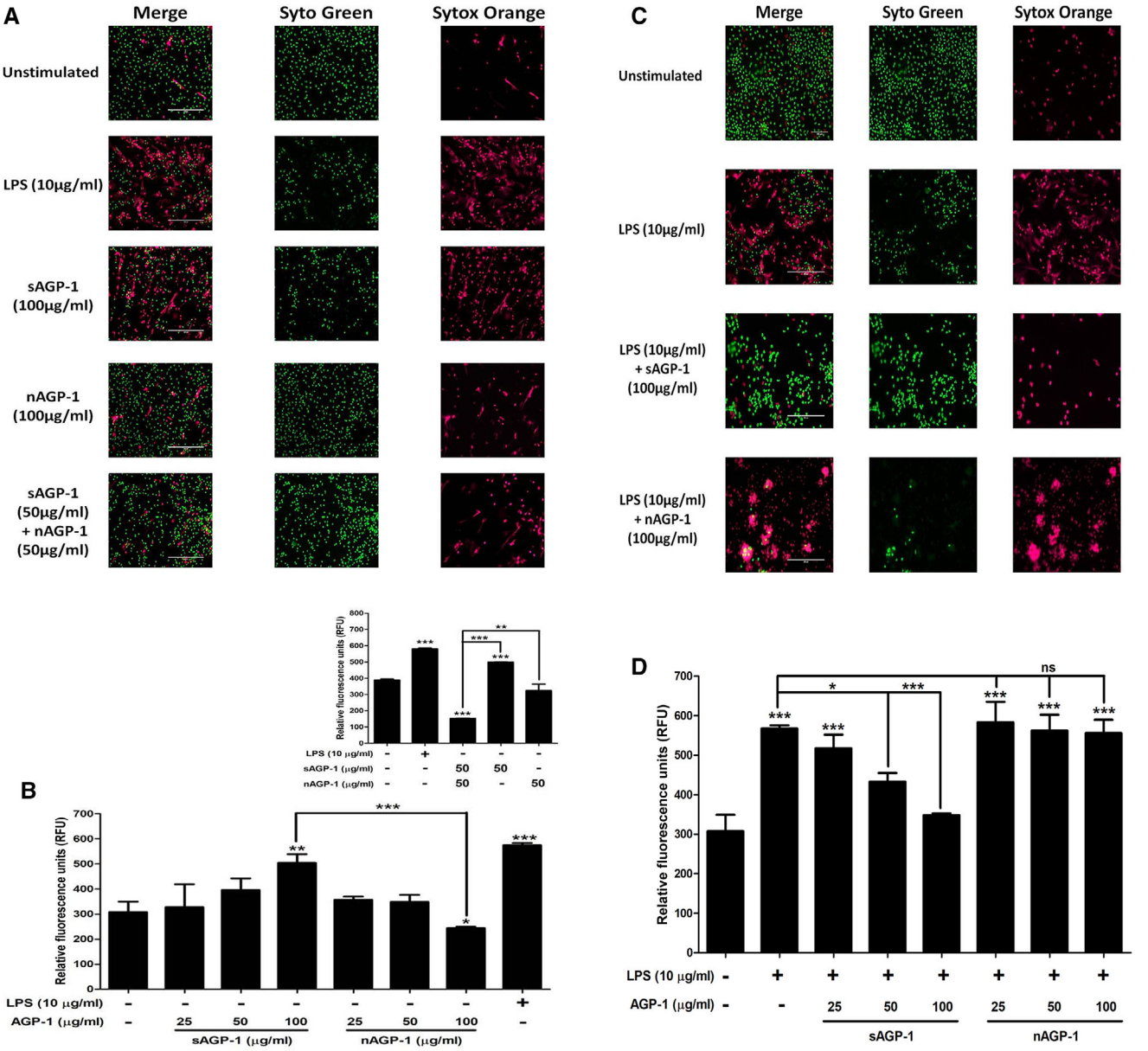

FIGURE 4 **sAGP-1, but not nAGP-1, induces NETosis**: (A) NET formation. Isolated human neutrophils adhering to poly-L-lysine-coated slides were incubated with media alone, or with sAGP-1, nAGP-1, and LPS for 1 h and were then stained with cell-permeable, Syto Green, and/ or with cell-impermeable Sytox orange to label polymeric DNA. NETs were assessed by live cell imaging using fluorescence microscope at 20× magnification (Scale: 200 μm). NET formation by LPS (red fluorescence) served as positive control. (B) Concentration–response relationships of NETosis. NETs were quantified using high-throughput method as explained in section "*Materials and Methods.*" Neutrophils were stimulated with sAGP-1, nAGP-1 (25, 50, and 100 μg/ml) or LPS for 1 h before quantifying NETs by fluorometry. In a parallel experiment, neutrophils were incubated with sAGP-1, nAGP-1, and combination of sAGP-1 and nAGP-1 (inset). LPS served as positive control. (C) Neutrophils were treated respectively with vehicle, LPS (10 μg/ml) in the presence/absence of sAGP-1 and nAGP-1 (25, 50, and 100 μg/ml). The mixture was incubated for 60 min at 37°C and stained with Syto green and Sytox orange fluorescent dye mixture. The NETs were visualized under a fluorescence microscope at a magnification of 20×. sAGP-1 inhibited TLR-4 (LPS)-mediated NETosis, whereas nAGP-1 did not have any effect on LPS-mediated effects. (D) NETosis was quantified using high-throughput method as explained under section "*Materials and Methods.*" The data shown are mean ± SEM. $^{***}P < 0.0001$, $^{**}P < 0.001$, and $^{*}P < 0.01$ as determined by one-way ANOVA

sAGP-1 (Figs. 7B–7F). These findings were confirmed by the results of 3 separate experiments that used platelets from different donors. The totality of these results shows congruence of the effect of sAGP-1 on aggregation, cAMP accumulation, kinase phosphorylation, and VASP phosphorylation across a range of agonist effectiveness.

4 | DISCUSSION

AGP-1 is an acute phase protein primarily secreted from hepatocytes, but also secreted from extra hepatic sites.[3–5] Our results demonstrate unique biologic effects of different glycoforms of the acute phase

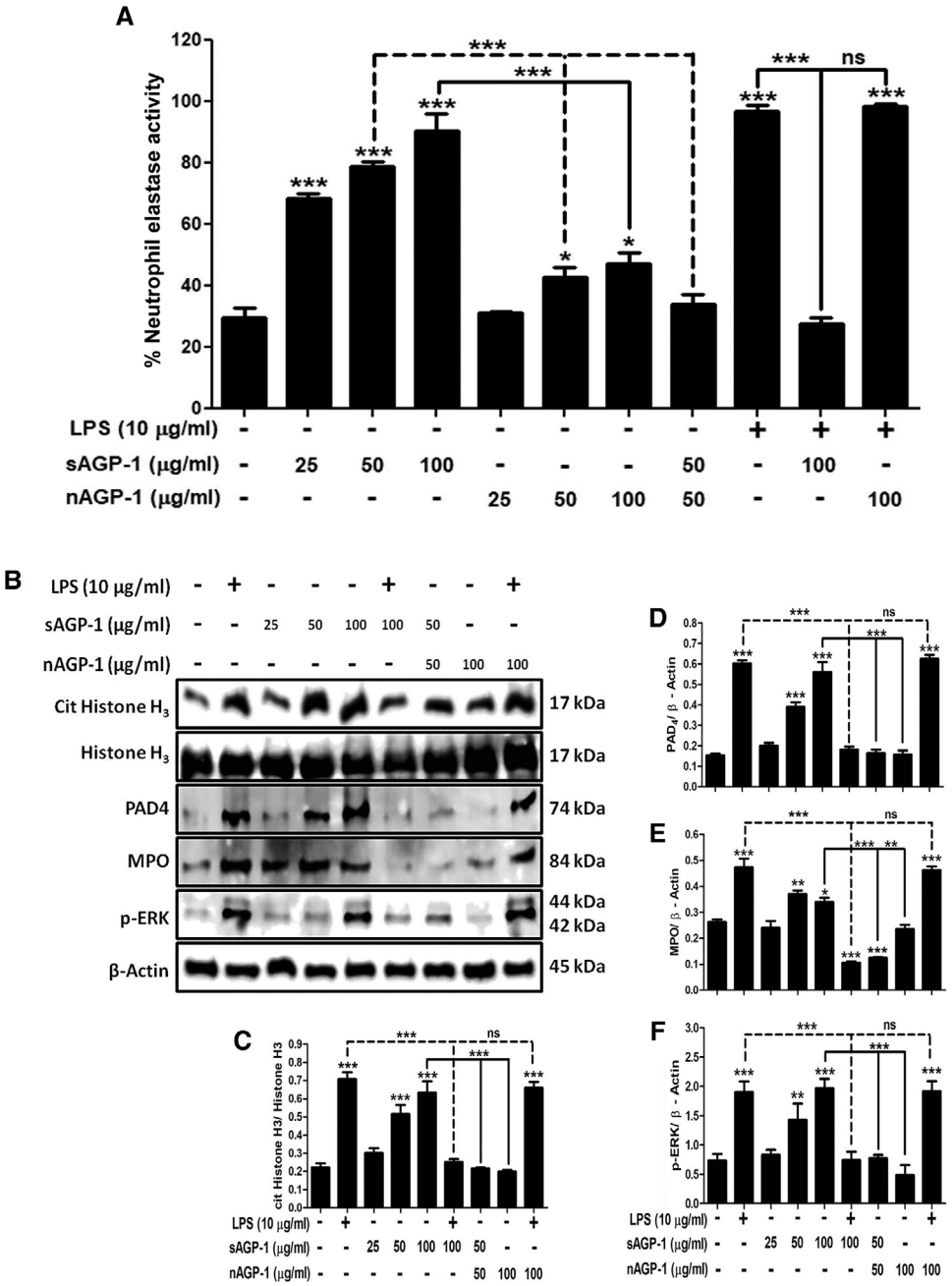

FIGURE 5 **Profiling of sAGP-1-induced NETosis**: (A) Quantification of NETosis. Apart from the high-throughput method, NETosis was also quantified by using NETosis assay kit. Neutrophils were stimulated with LPS (10 μg/ml), sAGP-1, and/or nAGP-1 (25, 50, and 100 μg/ml). In addition, neutrophils were also treated with combination of LPS (10 μg/ml), sAGP-1 (100 μg/ml), and/ or nAGP-1 (100 μg/ml) and submaximal concentration of sAGP-1 and nAGP-1 (50 μg/ml). (B) Immunoblots for markers of NETosis. Immunoblots for the key markers of NETosis like cit His H3, PAD4, MPO, and phospho-ERK was performed. sAGP-1-induced the expression of the key markers of NETosis in a concentration-dependent manner, whereas it inhibited LPS-induced expression of these proteins. Although, nAGP-1 failed to induce expression of these proteins even at highest concentration (100 μg/ml), submaximal concentration of nAGP-1 (50 μg/ml) inhibited sAGP-1 (50 μg/ml)-induced expression of cit His H3, PAD4, MPO, and phospho-ERK. (C–F) Densitometric analyses of NETosis immunoblots. Densitometric analysis of blots obtained from 3 experiments was done using ImageJ software (ver. 1.51j8). The data shown are mean ± SEM. $^{***}P < 0.0001$, $^{*}P < 0.01$ as determined by one-way ANOVA

glycoprotein AGP-1, depending on its origin in either serum (sAGP-1) or from activated neutrophils (nAGP-1). AGP-1 is often considered as one of the markers of several inflammatory diseases.[2,50] Although AGP-1 levels are elevated during inflammation, its biologic function(s) are not completely understood. As there are more than 150 glycoforms of AGP-1 present in the human plasma, this molecular diversity adds to the complexity of AGP-1 biology.[2,8,13,14,17] To this end, we isolated and characterized a novel AGP-1 glycoform from PAF-stimulated human neutrophils (nAGP-1). We were focused in particular on determining the functional differences between nAGP-1 and sAGP-1, if so, does it

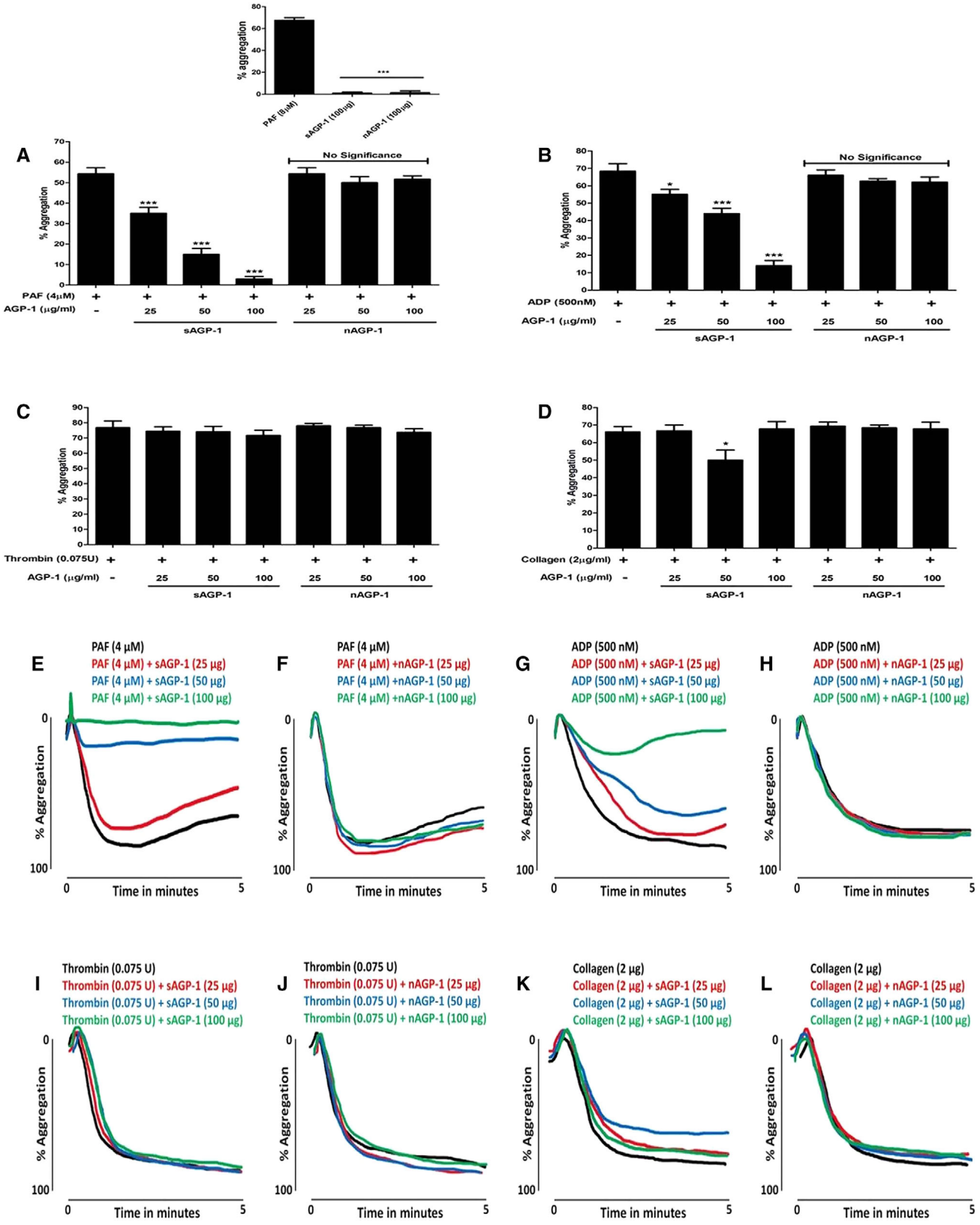

FIGURE 6 **sAGP-1, but not nAGP-1, inhibits stimulated platelet aggregation.** Platelet aggregation was induced by indicated amounts of PAF (A, E, and F), ADP (B, G, and H), thrombin (C, I, and J), or collagen (D, K, and L) with or without sAGP-1 and nAGP-1. (A) inset shows the effect of PAF (positive control), sAGP-1 and nAGP-1 on platelet aggregation. Each set of experiments were carried out with platelets from the same donor as well as repeated with platelets from at least 3 other donors. All assays were performed using Chrono-log aggregometer and the traces were recorded using AGGRO/LINK 8 ver.1.0.1 software. Representative trace of 3 independent experiments is shown here. The aggregation traces were merged using Wacom graphics pad. The data shown are mean ± SEM ($n = 3$). ***$P < 0.0001$, *$P < 0.01$ as determined by one-way ANOVA

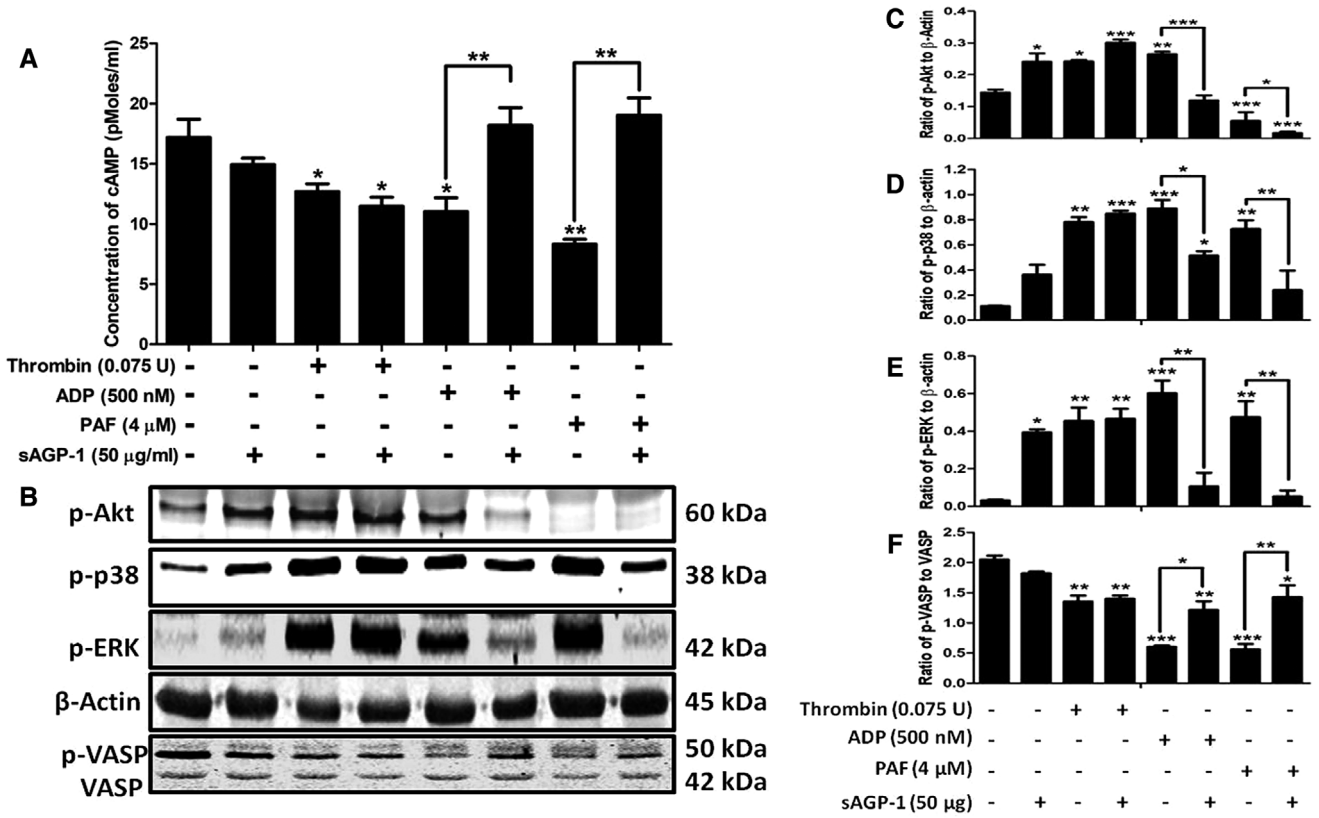

FIGURE 7 Inhibition of PAF and ADP-induced platelet aggregation by sAGP-1 is mediated by a cAMP-dependent pathway: (A) quantification of cAMP levels in platelets. Washed platelets were stimulated with PAF, ADP, or thrombin with or without sAGP-1. After incubation, the cells were collected by centrifugation and then assayed for cAMP by ELISA. The data represent results from 2 different experiments. (B) Phosphokinase Western blot. The phosphorylation status of the stated kinases treated, or not, with the indicated agonist as in the preceding panel was visualized by Western blotting. Phosphorylation of Akt, p38, ERK, or VASP was normalized using total β-actin. (C–F) Densitometric analyses of phosphokinase immunoblots. Densitometric analysis of blots obtained from 3 experiments was done using ImageJ software (ver. 1.51j8). The data shown are mean ± SEM. $^{***}P < 0.001$, $^{**}P < 0.01$, and $^{*}P < 0.05$ as analyzed by one-way ANOVA

play a role during inflammatory responses, a concept not yet examined in the field.

We determined whether an extrahepatic source of AGP-1 (neutrophils) was identical to sAGP-1 in structure and function, or whether the plethora of glycoforms also contributes to functional diversity. We found that unstimulated human neutrophils, the first responder of the innate immune system, secreted little AGP-1, but did so in response to any of neutrophil agonists. The AGP-1 released from PAF-stimulated neutrophils consisted primarily of 2 immunoreactive species with distinct electrophoretic mobilities. One glycoform migrated like sAGP-1 (43 kDa) (secreted in low concentration), whereas the major product when PAF was the stimulus was a slower migrating glycoform (~60 kDa). There are previous reports that a higher molecular weight AGP-1 exists in the secondary granules of both human and bovine neutrophils.[6,51] However, its structural details were not unraveled.

We found AGP-1 secretion from neutrophils in response to PAF varied with agonist concentration, where more AGP-1 was secreted with lower concentration of PAF. Although nAGP-1 (both ~60 kDa and 43 kDa glycoforms) eluted together in the void volume of Cibacron chromatography (data not shown), DEAE chromatography completely resolved both the slowly and rapidly migrating AGP-1 glycoforms. We discovered the difference in behavior between the glycoforms was the inability of the higher molecular weight (~60 kDa) nAGP-1 to bind positively charged DEAE resin but not the lower molecular weight nAGP-1 (43 kDa). The differences in behavior was not due to protein itself, as mass spectrometry evidence confirmed that the sAGP-1 retained by the DEAE column generated the same peptides after trypsin digestion as that of nAGP-1, and the same AGP-1 gene was identified by the Protein Discoverer program for both proteins. The differences between sAGP-1 and nAGP-1 were found to reside in N-glycans. Analyses revealed that the glycosylation of nAGP-1 is dramatically different from that of sAGP-1. nAGP-1 mainly expressed high-mannose, non-sialylated and monosialylated N-glycans, as opposed to sAGP-1, which expressed monosialylated and disialylated N-glycans. In accordance with this, nAGP-1, which only partially expresses monosialylated N-glycans, failed to bind to the positively charged DEAE resin.

Furthermore, higher molecular weight (~60 kDa) nAGP-1 after DEAE-purification showed faster mobility than that of the abundant 43 kDa sAGP-1 (Fig. 2C). Therefore, we hypothesized the presence of uncharacterized "AGP-1 binding factor" that may account for the slower electrophoretic mobility of nAGP-1 before purification as previously hypothesized by Libert et al.[52] This "AGP-1 binding factor"

might dissociate during the DEAE-purification step and hence the faster mobility of purified nAGP-1 (~35 kDa). Although we performed "add-back experiment" to regain the higher molecular weight fraction (~60 kDa) of nAGP-1, these experiments were unsuccessful (data not shown). It is possible that there may be more than one binding factor(s) with low abundance. The search for this uncharacterized "AGP-1 binding factor" is still ongoing. Thus, we conclude that both the slow (~60 kDa) and rapidly migrating (~35 kDa) nAGP-1 species are glycoforms of the same nAGP-1 protein. However, the less secreted 43 kDa AGP-1, due to its similarity with that of sAGP-1, might bind to the DEAE resin like that of sAGP-1. Hence, the nAGP-1 thus purified is homogenous. As the concentration of nAGP-1 secreted from the stimulated neutrophils is very less (~0.2–0.5 μg/10^6 neutrophils) compared with the abundance of sAGP in serum (~0.7 mg/ml), several rounds of purification for nAGP-1 were performed. The DEAE-purified nAGP-1 (~35 kDa) was pooled, characterized (for molecular weight and glycan structure) and used for the functional studies.

Our next question was whether AGP-1 glycoforms differ in their function. To address this, we first defined relevant functions for AGP-1 in the inflammatory system. Neutrophils when stimulated/activated migrate to the site of inflammation and undergo degranulation and produce ROS. The granules of neutrophils contains many antimicrobial proteins and peptides including but not limited to MPO, matrix metalloproteases, elastases, cathepsins, defensins, and so on.[53,54] We employed neutrophils, as activation of neutrophils and NETosis play a critical role in various inflammatory processes.[55–57] In accordance with our previous data, sAGP-1-induces concentration-dependent activation of neutrophil adhesion and migration, suggesting that the sAGP-1 induces Ca^{2+} influx to activate neutrophils.[58,59] Here, sAGP-1 is as effective as IL-8, but nAGP-1 is significantly less potent in activating either of these responses. In addition, sAGP-1 also induced degranulation of neutrophils (MPO secretion) and ROS production, whereas nGAP-1 was not an effective stimulator of neutrophils. Similarly, we found that although sAGP-1 stimulates NETosis, nAGP-1 does not. Moreover, nAGP-1 suppresses NETosis stimulated by sAGP-1, whereas sAGP-1, but not nAGP-1, suppresses NETosis induced by LPS. This effect might be due to direct interaction of AGP-1 with LPS thereby quenching LPS's effects as suggested by Huang et al.[60] To check this possibility, we performed binding studies using FITC conjugated LPS with sAGP-1. However, we could not see any significant binding of LPS to sAGP-1 (data not shown). Additionally, the carbohydrate moiety of nAGP-1 might physically prevent recognition of the carbohydrate structures displayed by sAGP-1 and LPS. NETosis is of 2 types; suicidal and vital. Regardless of the type, mechanism of NETosis generally follows the Raf-MEK-ERK pathway that involves ROS production by NADPH oxidase and MPO.[47–49,61,62] We found that sAGP-1, but not nAGP-1, induced increase in ROS production and also the expression of the MPO, PAD4, and phosphorylation of ERK in a concentration-dependent fashion, whereas LPS-induced expression of these proteins were inhibited by sAGP-1. Hence, we hypothesize that sAGP-1 may induce NETosis via Raf-MEK-ERK pathway, a hallmark of suicidal NETosis. We conclude that plasma sAGP-1 stimulates leukocyte function, whereas neutrophil-derived nAGP-1 mostly does not. This difference in biologic function reflects differences in post-translational modification of these proteins by glycans. Thus, stimulated neutrophils produce an anti-inflammatory glycoform of AGP-1 that counteracts the proinflammatory actions of circulating sAGP-1.

The variations in the effects of AGP-1 glycoforms are also extended to the responses of platelets, which play a critical role also in inflammation.[63–68] In fact, platelets are considered as immune cells, besides their role in hemostasis and blood coagulation.[69–71] Although neither glycoforms alone stimulated platelet aggregation, sAGP-1 proved to be a highly effective suppressor of platelets stimulated by PAF or ADP, less so for those stimulated by soluble collagen, and was without effect on the strong agonist thrombin. Again, nAGP-1 differed in function from sAGP-1 and had no effect on stimulated platelet aggregation. The concentration-dependent inhibitory effect of sAGP-1 on platelet function induced by PAF or ADP correlated to a sharp increase in intracellular cAMP levels. In contrast, thrombin-induced aggregation and cAMP levels were not affected by sAGP-1. Phosphorylation of VASP is dependent on cAMP and the PKA pathway it controls,[72,73] and sAGP-1 up-regulated phosphorylation of VASP in PAF- or ADP-stimulated platelets, but not in thrombin stimulated cells. sAGP-1 reduced PAF- and ADP-stimulated phosphorylation and activation of Akt, ERK, and p38 kinases, but again thrombin stimulation of these enzymes were unaffected by sAGP-1. These results, then, suggest that sAGP-1 inhibits platelet aggregation by weaker agonists via cAMP–PKA-mediated signaling (Fig. 8), supporting the claim that AGP-1 demonstrates antithrombotic effects.[28–30]

Previously, AGP-1 is shown to act via, a family of receptors called Sialic acid binding immunoglobulin like lectins (Siglec), Siglec-5. Siglec-5 receptor signaling, although not well understood, demonstrates both activating as well as inhibitory inflammatory signaling in neutrophils.[58,74–76] Moreover, we show the involvement of sAGP-1 in the cAMP pathway in platelets, which is a characteristic feature of GPCRs and not of the Siglec receptors.[27,77,78] Put together all these findings, we propose that sAGP-1 and nAGP-1 might act via different or related receptors and also that sAGP-1 might have different receptors on different cells.

In conclusion, our studies demonstrate that AGP-1 displays structural heterogeneity in its glycan structures associated with differences in physiologic functions. Isolation and characterization of a glycoform of AGP-1 released from PAF-stimulated human neutrophils represents a nonhepatic source of extracellular AGP-1, which is less proinflammatory than hepatic sAGP-1 on platelets and neutrophils. The basis for these differences is the distinct carbohydrate chain composition and structure incorporated by the 2 cell types rather than the AGP-1 protein itself. Furthermore, our studies demonstrate that the AGP-1 glycoform released from stimulated neutrophils in the early phases of inflammation is not an effective positive acute phase protein, but instead counteracts the hepatic sAGP-1 glycoform. These findings in part explain the contradictory role of AGP-1 in various inflammatory processes. This, in turn, identifies a need for future investigations to determine functions of the multitude of other AGP-1 glycoforms and there is a need to differentially quantify AGP-1 glycoforms rather than just AGP-1 protein in health and diseases, which can be an

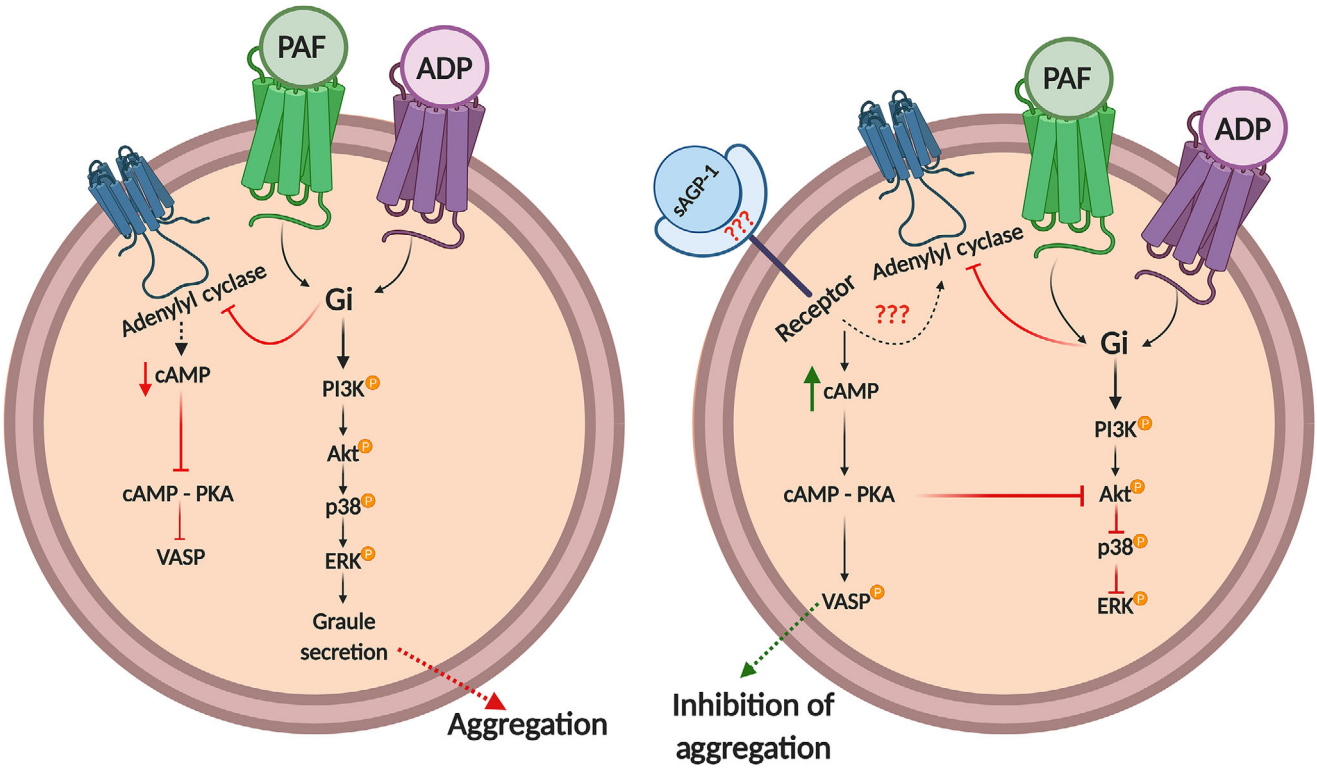

FIGURE 8 Proposed action of sAGP-1-induced inhibition of PAF- and ADP-mediated platelet aggregation: sAGP-1 up-regulates cAMP levels in PAF or ADP activated platelets, thereby activating PKA. This then activates VASP and inhibits Akt phosphorylation and activation thereby inhibiting downstream signaling and platelet aggregation. The illustration was created with BioRender.com

insurmountable task. The other greatest challenge lies in identifying appropriate receptors (Fig. 8) for AGP-1 glycoforms that ligate and alter intracellular signaling pathways.

AUTHORSHIP

G.K.M. conceived and designed experiments; M.S.S. designed and performed major experiments. K.V.A., S.P.J., B.K.M., and R.A.C. performed other minor experiments reported in the manuscript; G.K.M., A.S.W., M.T.R., C.C.Y., and T.M.M. analyzed the results. V.B. conducted and analyzed mass spectrometry; R.D.C. and S.L. performed and analyzed Glycomics data. G.K.M., M.T.R., T.M.M., S.L., R.D.C., and M.S.S. wrote and edited the manuscript.

ACKNOWLEDGMENTS

The authors thank Mr. Neal Tolley and Mr. Mark Cody, at the University of Utah Molecular Medicine Program in Salt Lake City, Utah, USA for their technical assistance and Prof. B.S. Vishwanath and Mr. Rudresha G.V, Dept. of Studies in Biochemistry, University of Mysore, Mysuru, India, for graciously sharing the antibodies. The authors also thank Prof. Guy Zimmerman, University of Utah, Salt Lake City, USA and Dr. Stephen Prescott, OMRF, Oklahoma, USA for their timely advice during the course of this study. The authors thank University Grants Commission (UGC), India [for Basic Science Research fellowship – F4-1/2006(BSR)/7-366/2012(BSR) to MSS, National Fellowship for Higher Education (NFHE-ST) – F1-17/2015-16/NFST-2015-17-ST-KAR-3879/(SA-III/Website) to KVA] and Vision Group of Science & Technology (VGST), Government of Karnataka, India to the Department of Studies in Biochemistry, University of Mysore, Mysuru, India, and the National Center for Functional Glycomics Grant P41GM103694 (RDC and SL). This work was funded by the NHLBI (HL092746, HL126547), NICHD (HD93826), and NIA (AG048022), and supported in part by Merit Review Award Number I01 CX001696 from the United States (U.S.) Department of Veterans Affairs Clinical Sciences R&D (CSRD) Service. This material is the result of work supported with resources and the use of facilities at the George E. Wahlen VA Medical Center, in Salt Lake City, Utah. The content is solely the responsibility of the authors and does not necessarily represent the official views of the National Institutes of Health or the U.S. Government.

DISCLOSURES

The authors declare no conflicts of interest.

ORCID

Gopal K Marathe https://orcid.org/0000-0002-0025-6677

REFERENCES

1. Schmid K, Mao S, Kimura A, Hayashi S, Binette JP. Isolation and characterization of a serine-threonine-rich galactoglycoprotein from normal human plasma. *J Biol Chem*. 1980;255:3221-3226.

2. Fournier T, Medjoubi-N N, Porquet D. Alpha-1-acid glycoprotein. *Biochim Biophys Acta Protein Struct Mol Enzymol*. 2000;1482:157-171.
3. Hochepied T, Berger FG, Baumann H, Libert C. α1-Acid glycoprotein: an acute phase protein with inflammatory and immunomodulating properties. *Cytokine Growth Factor Rev*. 2003;14:25-34.
4. Gendler SJ, Dermer GB, Silverman LM, Tökés ZA. Synthesis of α1-antichymotrypsin and α1-acid glycoprotein by human breast epithelial cells. *Cancer Res*. 1982;42:4567-4573.
5. Adam P, Sobek O, Táborský L, Hildebrand T, Tutterová O, Žáček P. CSF and serum orosomucoid (α-1-acid glycoprotein) in patients with multiple sclerosis: a comparison among particular subgroups of MS patients. *Clin Chim Acta*. 2003;334:107-110.
6. Theilgaard-Mönch K, Jacobsen LC, Rasmussen T, et al. Highly glycosylated α1-acid glycoprotein is synthesized in myelocytes, stored in secondary granules, and released by activated neutrophils. *J Leukoc Biol*. 2005;78:462-470.
7. Ceciliani F, Pocacqua V. The acute phase protein α1-acid glycoprotein: a model for altered glycosylation during diseases. *Curr Protein Pept Sci*. 2007;8:91-108.
8. Ongay S, Neusüβ C. Isoform differentiation of intact AGP from human serum by capillary electrophoresis–mass spectrometry. *Anal Bioanal Chem*. 2010;398:845-855.
9. Ceciliani F, Lecchi C. The immune functions of α1 acid glycoprotein. *Curr Protein Pept Sci*. 2019;20:505-524.
10. Moule SK, Peak M, Thompson S, Turner GA. Studies of the sialylation and microheterogeneity of human serum α1-acid glycoprotein in health and disease. *Clin Chim Acta*. 1987;166:177-185.
11. Mackiewicz A, Marcinkowska-Pieta R, Ballou S, Mackiewicz S, Kushner I. Microheterogeneity of alpha1-acid glycoprotein in the detection of intercurrent infection in systemic lupus erythematosus. *Arthritis Rheum*. 1987;30:513-518.
12. De Graaf TW, Van der Stelt M, Anbergen M, Van Dijk W. Inflammation-induced expression of sialyl Lewis X-containing glycan structures on alpha 1-acid glycoprotein (orosomucoid) in human sera. *J Exp Med*. 1993;177:657-666.
13. Pawlowski T, Mackiewicz SH, Mackiewicz A. Microheterogeneity of alpha1-acid glycoprotein in the detection of intercurrent infection in patients with rheumatoid arthritis. *Arthritis Rheum*. 1989;32:347-351.
14. Van Dijk W, Havenaar E, Brinkman-Van der Linden EC. α 1-acid glycoprotein (orosomucoid): pathophysiological changes in glycosylation in relation to its function. *Glycoconj J*. 1995;12:227-233.
15. Zhang D, Huang J, Luo D, Feng X, Liu Y. Glycosylation change of alpha-1-acid glycoprotein as a serum biomarker for hepatocellular carcinoma and cirrhosis. *Biomark Med*. 2017;11:423-430.
16. Xiao K, Su L, Yan P, et al. α-1-Acid glycoprotein as a biomarker for the early diagnosis and monitoring the prognosis of sepsis. *J Crit Care*. 2015;30:744-751.
17. Van Dijk W, Brinkman-Van der Linden EC, Havenaar EC. Glycosylation of α1-acid glycoprotein (orosomucoid) in health and disease. *Trends Glycosci Glycotechnol*. 1998;10:235-245.
18. Hochepied T, Van Molle W, Berger FG, Baumann H, Libert C. Involvement of the acute phase protein α1-acid glycoprotein in nonspecific resistance to a lethal gram-negative infection. *J Biol Chem*. 2000;275:14903-14909.
19. Libert C, Brouckaert P, Fiers W. Protection by alpha 1-acid glycoprotein against tumor necrosis factor-induced lethality. *J Exp Med*. 1994;180:1571-1575.
20. Costello M, Fiedel BA, Gewurz H. Inhibition of platelet aggregation by native and desialised alpha-1 acid glycoprotein. *Nature*. 1979;281:677-678.
21. Nakamura K, Ito I, Kobayashi M, Herndon DN, Suzuki F. Orosomucoid 1 drives opportunistic infections through the polarization of monocytes to the M2b phenotype. *Cytokine*. 2015;73:8-15.
22. Mestriner FL, Spiller F, Laure HJ, et al. Acute-phase protein alpha-1-acid glycoprotein mediates neutrophil migration failure in sepsis by a nitric oxide-dependent mechanism. *Proc Nat Acad Sci USA*. 2007;104:19595-19600.
23. Higuchi H, Kamimura D, Jiang JJ, et al. Orosomucoid 1 is involved in the development of chronic allograft rejection after kidney transplantation. *Int Immunol*. 2020;32:335-346.
24. Andersen P. The antiheparin effect of α1-acid glycoprotein, evaluated by the activated partial thromboplastin time and by a factor Xa assay for heparin. *Pathophysiol Haemos Thromb*. 1980;9:303-309.
25. Berntsson J, Östling G, Persson M, Smith JG, Hedblad B, Engström G. Orosomucoid, carotid plaque, and incidence of stroke. *Stroke*. 2016;47:1858-1863.
26. Boncela J, Papiewska I, Fijalkowska I, Walkowiak B, Cierniewski CS. Acute phase protein α1-acid glycoprotein interacts with plasminogen activator inhibitor type 1 and stabilizes its inhibitory activity. *J Biol Chem*. 2001;276:35305-35311.
27. Gunnarsson P, Levander L, Påhlsson P, Grenegård M. α1-acid glycoprotein (AGP)-induced platelet shape change involves the Rho/Rho kinase signalling pathway. *Thromb Haemost*. 2009;102:694-703.
28. Fiedel B, Costello M, Gewurz H, Hussissian E. Effects of heparin and α1-acid glycoprotein on thrombin or activated thrombofax reagent-induced platelet aggregation and clot formation. *Pathophysiol Haemos Thromb*. 1983;13:89-95.
29. Osikov M, Makarov E, Krivokhizhina L. Effects of α 1-acid glycoprotein on hemostasis in experimental septic peritonitis. *Bull Exp Biol Med*. 2007;144:178-180.
30. Daemen MA, Heemskerk VH, van't Veer C, et al. Functional protection by acute phase proteins α1-acid glycoprotein and α1-antitrypsin against ischemia/reperfusion injury by preventing apoptosis and inflammation. *Circulation*. 2000;102:1420-1426.
31. Stark RJ, Aghakasiri N, Rumbaut RE. Platelet-derived Toll-like receptor 4 (Tlr-4) is sufficient to promote microvascular thrombosis in endotoxemia. *PLoS One*. 2012;7:e41254.
32. Rondina M, Schwertz H, Harris E, et al. The septic milieu triggers expression of spliced tissue factor mRNA in human platelets. *J Thromb Haemost*. 2011;9:748-758.
33. Jia S-J, Niu P-P, Cong J-Z, Zhang B-K, Zhao M. TLR4 signaling: a potential therapeutic target in ischemic coronary artery disease. *Int Immunopharmacol*. 2014;23:54-59.
34. Schattner M. Platelet TLR4 at the crossroads of thrombosis and the innate immune response. *J Leukoc Biol*. 2019;105:873-880.
35. Sumanth MS, Abhilasha KV, Jacob SP, et al. Acute phase protein, alpha - 1- acid glycoprotein (AGP-1), has differential effects on TLR-2 and TLR-4 mediated responses. *Immunobiology*. 2019;224:672-680.
36. Lakshmikanth CL, Jacob SP, Kudva AK, et al. Escherichia coli Braun Lipoprotein (BLP) exhibits endotoxemia–like pathology in Swiss albino mice. *Sci Rep*. 2016;6:34666.
37. Watanabe J, Marathe GK, Neilsen PO, et al. Endotoxins stimulate neutrophil adhesion followed by synthesis and release of platelet-activating factor in microparticles. *J Biol Chem*. 2003;278:33161-33168.
38. Lowry OH, Rosebrough NJ, Farr AL, Randall RJ. Protein measurement with the Folin phenol reagent. *J Biol Chem*. 1951;193:265-275.
39. Strohalm M, Kavan D, Novak P, Volny M, Havlicek V. mMass 3: a cross-platform software environment for precise analysis of mass spectrometric data. *Anal Chem*. 2010;82:4648-4651.
40. Bradley PP, Priebat DA, Christensen RD, Rothstein G. Measurement of cutaneous inflammation: estimation of neutrophil content with an enzyme marker. *J Invest Dermatol*. 1982;78:206-209.
41. Yoshikawa T, Furukawa Y, Murakami M, Watanabe K, Kondo M. Effect of vitamin E on endotoxin-induced disseminated intravascular coagulation in rats. *Thromb Haemost*. 1982;47:235-237.
42. Carmona-Rivera C, Kaplan MJ. Induction and quantification of NETosis. *Curr Protoc Immunol*. 2016;115:14.41.01-14.41.14.

43. Zhou L, Schmaier AH. Platelet aggregation testing in platelet-rich plasma: description of procedures with the aim to develop standards in the field. *Am J Clin Pathol*. 2005;123:172-183.
44. Leick M, Azcutia V, Newton G, Luscinskas FW. Leukocyte recruitment in inflammation: basic concepts and new mechanistic insights based on new models and microscopic imaging technologies. *Cell Tissue Res*. 2014;355:647-656.
45. McIntyre TM, Prescott SM, Weyrich AS, Zimmerman GA. Cell-cell interactions: leukocyte-endothelial interactions. *Curr Opin Hematol*. 2003;10:150-158.
46. Mesa MA, Vasquez G. NETosis. *Autoimmune Dis*. 2013;2013:651497.
47. Desai J, Kumar SV, Mulay SR, et al. PMA and crystal-induced neutrophil extracellular trap formation involves RIPK1-RIPK3-MLKL signaling. *Eur J Immunol*. 2016;46:223-229.
48. Hakkim A, Fuchs TA, Martinez NE, et al. Activation of the Raf-MEK-ERK pathway is required for neutrophil extracellular trap formation. *Nat Chem Biol*. 2011;7:75-77.
49. Li P, Li M, Lindberg MR, Kennett MJ, Xiong N, Wang Y. PAD4 is essential for antibacterial innate immunity mediated by neutrophil extracellular traps. *J Exp Med*. 2010;207:1853-1862.
50. Komori H, Watanabe H, Shuto T, et al. α1-acid glycoprotein up-regulates CD163 via TLR4/CD14 pathway: possible protection against hemolysis-induced oxidative stress. *J Biol Chem*. 2012;287:30688-30700.
51. Rahman MM, Miranda-Ribera A, Lecchi C, et al. Alpha1-acid glycoprotein is contained in bovine neutrophil granules and released after activation. *Vet Immunol Immunopathol*. 2008;125:71-81.
52. Libert C, Hochepied T, Berger FG, Baumann H, Fiers W, Brouckaert P. High-level constitutive expression of α1-acid glycoprotein and lack of protection against tumor necrosis factor-induced lethal shock in transgenic mice. *Transgenic Res*. 1998;7:429-435.
53. Borregaard N, Cowland JB. Granules of the human neutrophilic polymorphonuclear leukocyte. *Blood*. 1997;89:3503-3521.
54. Lacy P. Mechanisms of degranulation in neutrophils. *Allergy Asthma Clin Immunol*. 2006;2:98.
55. Iba T, Levy J. Inflammation and thrombosis: roles of neutrophils, platelets and endothelial cells and their interactions in thrombus formation during sepsis. *J Thromb Haemost*. 2018;16:231-241.
56. Kapoor S, Opneja A, Nayak L. The role of neutrophils in thrombosis. *Thromb Res*. 2018;170:87-96.
57. Perdomo J, Leung HH, Ahmadi Z, et al. Neutrophil activation and NETosis are the major drivers of thrombosis in heparin-induced thrombocytopenia. *Nat Commun*. 2019;10:1-14.
58. Gunnarsson P, Levander L, Påhlsson P, Grenegard M. The acute-phase protein α1-acid glycoprotein (AGP) induces rises in cytosolic Ca2+ in neutrophil granulocytes via sialic acid binding immunoglobulin-like lectins (Siglecs). *FASEB J*. 2007;21:4059-4069.
59. Levander L, Gunnarsson P, Grenegård M, Rydén I, Påhlsson P. Effects of α1-acid glycoprotein fucosylation on its Ca2+ mobilizing capacity in neutrophils. *Scand J Immunol*. 2009;69:412-420.
60. Huang JX, Azad MA, Yuriev E, et al. Molecular characterization of lipopolysaccharide binding to human α-1-acid glycoprotein. *J Lipids*. 2012;2012:475153.
61. Fuchs TA, Abed U, Goosmann C, et al. Novel cell death program leads to neutrophil extracellular traps. *J Cell Biol*. 2007;176:231-241.
62. Masuda S, Nakazawa D, Shida H, et al. NETosis markers: quest for specific, objective, and quantitative markers. *Clin Chim Acta*. 2016;459:89-93.
63. Rondina MT, GUO L. The era of thromboinflammation: platelets are dynamic sensors and effector cells during infectious diseases. *Front Immunol*. 2019;10:2204.
64. Rondina MT, Weyrich AS, Zimmerman GA. Platelets as cellular effectors of inflammation in vascular diseases. *Circ Res*. 2013;112:1506-1519.
65. Klinger MH. Platelets and inflammation. *Anat Embryol*. 1997;196:1-11.
66. Weyrich A, Lindemann S, Zimmerman G. The evolving role of platelets in inflammation. *J Thromb Haemost*. 2003;1:1897-1905.
67. Thomas MR, Storey RF. The role of platelets in inflammation. *Thromb Haemost*. 2015;114:449-458.
68. Dewitte A, Lepreux S, Villeneuve J, et al. Blood platelets and sepsis pathophysiology: a new therapeutic prospect in critical ill patients?. *Ann Intensive Care*. 2017;7:115.
69. Semple JW, Italiano JE, Freedman J. Platelets and the immune continuum. *Nat Rev Immunol*. 2011;11:264-274.
70. Ali RA, Wuescher LM, Worth RG. Platelets: essential components of the immune system. *Curr Trends Immunol*. 2015;16:65.
71. Morrell CN, Aggrey AA, Chapman LM, Modjeski KL. Emerging roles for platelets as immune and inflammatory cells. *Blood*. 2014;123:2759-2767.
72. Anton KA, Sinclair J, Ohoka A, et al. PKA-regulated VASP phosphorylation promotes extrusion of transformed cells from the epithelium. *J Cell Sci*. 2014;127:3425-3433.
73. Zhang Y-T, Xu L-H, Lu Q, et al. VASP activation via the Gα13/RhoA/PKA pathway mediates cucurbitacin-B-induced actin aggregation and cofilin-actin rod formation. *PLoS One*. 2014;9:e93547.
74. Ali SR, Fong JJ, Carlin AF, et al. Siglec-5 and Siglec-14 are polymorphic paired receptors that modulate neutrophil and amnion signaling responses to group B Streptococcus. *J Exp Med*. 2014;211:1231-1242.
75. Avril T, Freeman SD, Attrill H, Clarke RG, Crocker PR. Siglec-5 (CD170) can mediate inhibitory signaling in the absence of immunoreceptor tyrosine-based inhibitory motif phosphorylation. *J Biol Chem*. 2005;280:19843-19851.
76. Pepin M, Mezouar S, Pegon J, et al. Soluble Siglec-5 associates to PSGL-1 and displays anti-inflammatory activity. *Sci Rep*. 2016;6:37953.
77. Sadana R, Dessauer CW. Physiological roles for G protein-regulated adenylyl cyclase isoforms: insights from knockout and overexpression studies. *Neurosignals*. 2009;17:5-22.
78. Sassone-Corsi P. The cyclic AMP pathway. *Cold Spring Harb Perspect Biol*. 2012;4:a011148.

How to cite this article: Sumanth MS, Jacob SP, Abhilasha KV, et al. Different glycoforms of alpha-1-acid glycoprotein contribute to its functional alterations in platelets and neutrophils. *J Leukoc Biol*. 2021;109:915–930. https://doi.org/10.1002/JLB.3A0720-422R